J Incl Phenom Macrocycl Chem (2015) 83:119–129
DOI 10.1007/s10847-015-0547-2

ORIGINAL ARTICLE

Study on the separation of ofloxacin enantiomers by hydroxyl-propyl-β-cyclodextrin as a chiral selector in capillary electrophoresis: a computational approach

FakhrEldin O. Suliman[1] · Abdalla A. Elbashir[2] · Oliver J. Schmitz[3]

Received: 2 May 2015 / Accepted: 18 July 2015 / Published online: 28 July 2015

Abstract Hydroxypropyl-β-cyclodextrin (HPβCD) has been used successfully as a chiral additive to separate ofloxacin (OFL) enantiomers in a capillary electrophoresis system. Using electrospray-mass spectrometry (ESI–MS) it was revealed that OFL forms an inclusion complex with HPβCD at 1:1 stoichiometry. The interaction of the enantiomers with the host was further investigated by molecular modeling using molecular mechanics dockings, PM7 semiempirical calculations and molecular dynamics simulations. Calculations using PM7 semiempirical methods indicated that the separation is brought about by a large difference in the binding energies (ΔΔE) of 15 kcal mol^{-1} between R-OFL-HPβCD and S-OFL-HPβCD inclusion complexes. S-OFL was predicted to be eluted first by the PM7 method which corroborates the experimental results. Moreover, the molecular dynamic simulations show that the formation of stable R-OFL-HPβCD is because it is more deeply inserted into the cavity of the host. The study also revealed the absence of the role of strong hydrogen bonding in the enantioseparations.

✉ FakhrEldin O. Suliman
fsuliman@squ.edu.om

Abdalla A. Elbashir
hajaae@yahoo.com

Oliver J. Schmitz
oliver.schmitz@uni-due.de

[1] Department of Chemistry, College of Science, Sultan Qaboos University, Box 36, Al-Khod 123, Muscat, Oman

[2] Department of Chemistry, Faculty of Science, University of Khartoum, Box 321, Khartoum, Sudan

[3] Applied Analytical Chemistry, Faculty of Chemistry, University of Duisburg-Essen, Essen, Germany

Keywords Ofloxacin · Enantioseparation · Capillary electrophoresis · Molecular dynamics · PM7

Introduction

It is now well recognized that enantiomers biological activities vary greatly. Therefore, a great deal of attention is lately directed towards the stereochemistry of pharmaceuticals, agrochemicals, additives, and many other chemicals. Additionally, the pressing demand for pure chiral compounds has led to the development of various synthetic and separation procedures. Due to its high efficiency, simplicity, and versatility capillary electrophoresis (CE) technique has emerged as an appealing choice for enantioseparations, where small amount of samples and additives are used [1–5]. Customarily, in CE addition of chiral selectors to the background electrolyte (BGE) facilitated resolution of a huge number of chiral compounds. A glance at the literature can easily reveal the fact that macrocycle antibiotics and cyclodextrins are the most dominantly utilized running buffer additives [1, 3, 5–12]. So far the general mechanism adopted for the chiral resolution is the one based on the formation of transient diastereoisomers that exhibit different thermodynamic stability with an ensuing difference in migration times. Migration of ions in CE is governed by the mass-to-charge ratio of these ions. Therefore, the mobilities of free enantiomers are expected to be equal. However, complexation of these enantiomers may result in differences in shapes and net charges of the formed complexes due to the subtle differences in the fit of the guest molecules inside the cavity of the host [13–18]. Moreover, the time spent by enantiomer molecules inside the host is related to the

strength of intermolecular interactions between the host and guests.

Cyclodextrins (CDs) are cyclic oligosaccharides composed of 6, 7, or 8 glucopyranose α-(1-4)-linked units producing α-, β-, and γ-CD. These compounds and their modified derivative have found wide applications in chiral separations as chiral stationary phases as well as chiral additives.

Recently, theoretical modeling has been extensively used in the investigation of the inclusion complexes of CDs with various guest molecules. The methods employed include molecular mechanics, molecular dynamics, semiempirical methods and density functional theory calculations [4, 18–26]. Semiempirical methods are attracting lots of attention in the simulation of CD-inclusion compounds due to their reasonable accuracy and less computational demands. These studies were directed to unravel the nature of interaction between the host and the guest molecules to help in understanding the mechanism of complexation [4, 18, 22–25, 27–31]. These calculations have also been used to investigate the mechanistic characteristics of chiral recognition using supramolecular systems. Optimization of the inclusion complexes using quantum mechanical methods followed by MD simulations indicated that the differences in stabilities of inclusion complexes of enantiomers with the host where hydrogen bonding plays a crucial role lead to more efficient chiral separations [22].

Ofloxacin [(±)-9-fluoro-2, 3-dihydro-3-methyl-10-(4-methyl-1-piperazinyl)-7-oxo-7Hpyrido[1,2,3-de]-1,4-benzoxazine-6-carboxylic acid (Fig. 1)], (OFL), is a member of the fluoroquinolone antibiotics which exhibit a broad spectrum of activity against gram-positive and gram-negative bacteria. The antimicrobial activities of the two enantiomers of OFL are markedly different with the S-isomers exhibiting more than hudered times more potency compared to the R-isomer. The separation of the two enantiomers of OFL is reported in the literature using various techniques [2, 10, 32–35].

Interaction of OFL with various CDs has been recently investigated using different experimental techniques and also using molecular modeling [32]. Despite the detailed experimental study of the resolution of the enantiomers of OFL by CDs and the determination of complexation constants the mechanism of enantioseparation of OFL received little attention. The molecular mechanics approach used has not been applied to gain any atomistic insight into the chiral mechanism.

Investigation of the main factors responsible for complexation of the two enantiomers of OFL with HPβCD is, therefore, required to help delineate how the enantioseparation was achieved. Moreover, determination of the differences in intermolecular forces and energies of the guest–host systems allows better understanding of the separation mechanism and can assist in predicting the suitable chiral selector for a given enantioseparation system.

In this paper, the interaction of OFL with the HPβCD in aqueous solutions was examined using molecular dynamic (MD) simulations for five nanoseconds. In this regard our aim was focused on investigating specific interactions such as hydrogen bonding between the host and the guest molecules in aqueous media especially the role of CH–O bonds as secondary hydrogen bonding forces. The presence of such minor interactions may have a vital impact on the chiral separation [22]. Furthermore, more reliable thermodynamic parameters of the complexes were estimated using the newly introduced PM7 semiempirical method [36].

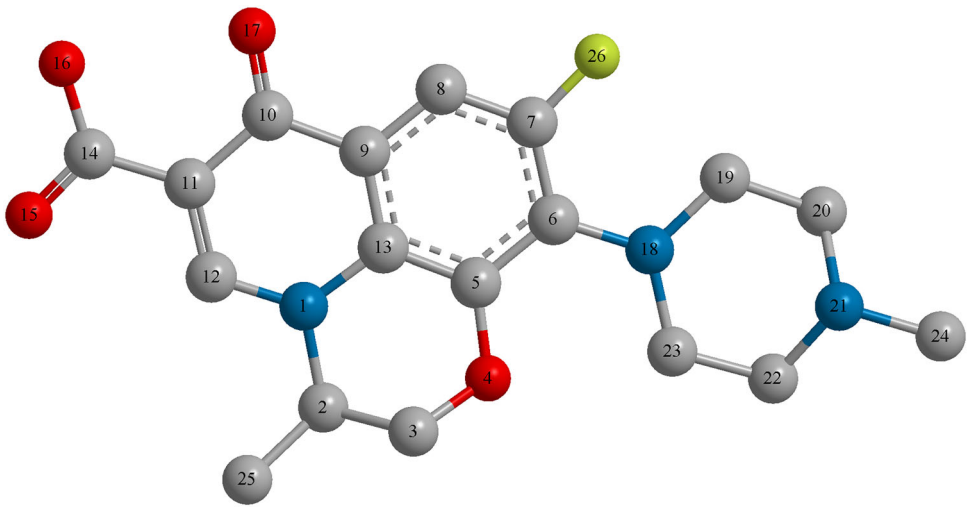

Fig. 1 Optimized structure of ofloxacin

Materials and methods

Reagents

Phosphoric acid (85 % w/w), sodium dihydrogen phosphate and the racemic mixture and the optically active forms of the OFL were purchased from Sigma-Aldrich (St Louis, MO, USA). β-Cyclodextrin (βCD) and 2-hydroxylpropyl β-cyclodextrins (HPβCD) were obtained from Fluka (Buchs, Switzerland). The phosphate buffer solutions were prepared using 50 mM sodium dihydrogen phosphate solution and the desired pH was adjusted by phosphoric acid. All drug samples were prepared in aqueous media at a concentration of 0.5 mg mL^{-1}. The concentrations of the chiral selectors, βCD and HPβCD were prepared by dissolving the pure materials in phosphate buffer.

CE Instrument and conditions

A Beckman P/ACE MDQ CE system equipped with a UV detector was used for all electrophoretic separations. A 50 mm ID fused-silica capillary from Polymicro Technologies (Phoenix, AZ, USA) of 40 cm length (30 cm from inlet to the detector window) was used and thermostated at 25 °C. The capillary was first conditioned with 1.0 mol L^{-1} HCl, 1.0 mol L^{-1} NaOH and methanol for 2 min each as described in the P/ACE MDQ CE instrumental manual. Then the capillary was rinsed with deionized water for 2 min at a pressure of 50 psi and equilibrated with background electrolyte (BGE) buffer before sample analysis. Samples were injected by pressure at 0.5 psi for 5 s, and separations were performed under 15 kV for 25 min with a positive high voltage. The data were collected and processed by Beckman P/A CE 32 Karat software Version 4.0. The capillary was rinsed 2 min with 0.1 mol L^{-1} NaOH, water, and BGE after each run. The resolution (Rs) are calculated according to the following equations: $Rs = 2(t_2 - t_1)/(w_1 + w_2)$. Where t_1, t_2, w_1, and w_2 are the migration times and peak widths at baseline for enantiomers 1 and 2, respectively.

ESI–MS

The mass spectra was obtained using Quattro-Ultima LC–MS system (Waters Corporation, Milford, USA) equipped with electrospray ionization (ESI) interface and operated by MassLynx software. The MS conditions were as follows: source temperature 100 °C, desolvation temperature 120 °C, desolvation flow rate 650 L min^{-1}, cone voltage 35 V, and capillary voltage setting 2.3 kV. The low and high mass resolution were set at 14.0 (arbitrary units), and the multiplier voltage was set at 650 V. Mixtures of OFL and HPβCD solutions (1–5 mM) dissolved in water are infused at 20 μL min^{-1} into the mass spectrometer.

Molecular modeling

The starting structures of R- and S-ofloxacin (R-, S-OFL) as well as β-cyclodextrin were extracted from the crystallographic parameters provided by the Structural Data Base System of the Cambridge crystallographic data center. All molecules were fully optimized with the semiempirical method PM7 [36] using the MOPAC2012 package (www.openmopac.net). Further, the structure of 2-hydroxypropyl-β-cyclodextrin (HPβCD) was built on the β-cyclodextrin structure by substitutions of 2-hydroxypropyl moieties randomly at O2 and O6 positions as a representation for the HPβCD mixtures.

To obtain the most stable complex between R- and S-OFL and the host molecule molecular docking studies were performed using *Autodock* program (version 4.2) [37]. In this work a Lamarckian genetic algorithm (LGA) for the docking study was used to generate the inclusion complexes. *Autodock* usually defines a conformational space by implementation of grids over all the possible search space. Grid maps of 58 × 58 × 58 Å grid box with 0.375 Å spacing were obtained using *Autogrid 4* program. The center of mass of the HPβCD was set as the center of the box. The initial torsions and positions of R- or S-OFL were generated randomly. With the help of *Autodock* tools the partial charges were calculated using the Gasteiger-Marsili method [38, 39]. For the search we used a population of 100 LGA runs with a maximum number of energy evaluations of 2.5×10^7 and a maximum number of generations of 27,000. An elitism value of 1 was used and a probability of mutation and cross-over of 0.02 and 0.08 were used respectively. At the end of each run the solutions are separated into clusters based on their lowest root mean square deviation (RMSD) and the best score based on a free energy function. Cluster solutions with average scores that are over 1.0 kcal mol^{-1} with respect to the best energy obtained in the respective run were selected.

The final structures obtained were refined and optimized by the semiempitrical PM7 method using the MOPAC2012. Using the same method thermodynamic parameters of the inclusion were estimated at a pressure of 1 atm and a temperature of 298 K.

In this work each system consisting of a guest and host molecule was solvated in a sphere of TIP3P water molecules [40] using periodic boundary conditions. Langevin dynamics were implemented to maintain the temperature and the pressure close to 300 K and 1 atm, respectively. The solvated complexes were equilibrated and energy minimized prior to MD simulations. Solvated complexes were heated to 300 K followed by an equilibration step of

500 ps at 300 K and 1 atm. MD production runs were performed at constant temperature and pressure for an additional 5 ns. The dynamics were performed using NAMD package [41], using CHARMM22 parametrization [42]. The time step for MD simulation was 2 fs. The initial gemoetries, topologies and force-field parameter files were generated by VEGA ZZ software [43], which was also used for the analysis of the MD trajectories. Also VMD software [44] was also used to perform analysis of the trajectories.

Results and discussion

Electrophoretic separation of OFL enantiomers

CDs have been widely used for chiral separation of racemic drugs. In this study β-CD and HPβCD were applied for the chiral separation of OFL enantiomers. As shown in Fig. 2a no chiral recognition was observed in the presence of (5–15 mM) β-CD. It is worth mentioning here that higher concentrations were not attempted due to the limited solubility of β-CD. However, when HPβCD was added to the running buffer as chiral selector enantioseparation was achieved as shown in Fig. 2b. Therefore HPβCD was used throughout the experiments. It is observed that the S-enantiomer was eluted first and this was further confirmed by spiking with the S-enantiomer standard.

The effect of pH on the resolution (R_s) of OFL enantiomers was investigated over the pH range 2.0–4.5, using 50 mM buffer solutions prepared at different pH containing 40 mM HP-β-CD. The results, illustrated in Fig. 3, show that a decrease in resolution was observed when the pH values were increased. Similar results were reported previously for OFL [32, 35].

ESI–MS

Using negative mode ESI–MS, the stoichiometry of the inclusion complexes of OFL and HPβCD were also investigated using different molar ratios. A typical mass spectrum of these mixtures is shown in Fig. 4. In this figure two clusters of peaks are clearly observed with distribution of masses. The first cluster of peaks with m/z 1366.3–1696.7 corresponds to HPβCD. These peaks are separated by 58 mass units which is equivalent to the mass of 2-hydroxypropyl units. The bell shaped distribution of these peaks represents HPβCD species with 4–10 hydroxypropyl substituents per βCD molecule. This is indicative of the random nature of the substitution process. The peaks marked with a strike correspond to m/z shift ~36 mass units representing chloride adducts.

The 1:1 inclusion complex shows a similar bell-shaped distribution pattern. It is clear from this figure that the various homologs of HPβCD forms 1:1 inclusion complex. However, the peak that corresponds to the inclusion complex between OFL with HPβCD containing four 2-hydroxypropyl substituents is either extremely small or not observed. Moreover, chloride adducts of the inclusion complex are also not observed.

Molecular modeling

It is known that a precise description of the structure of chemically modified cyclodextrins such as HPβCD is not realistic because of the wide range of random substitution patterns occurring during derivatization. HPβCD is customarily sysnthesized via condensation reaction between propylene oxide and βCD. Depending on the alkalinity different substituents at O2 and O6 positions of βCD are obtained [45]. In this work we selected a HPβCD species with two substituents at O2 and four substituents at O6 positions. The obtained structure was fully optimized by the newly introduced semiempirical method PM7.

The acid base properties of OFL and other fluoroquinolones have been described in the literature [46, 47]. The presence of a carboxylic acid group (pKa 6.2) at C11 (Fig. 1) and a piperazinyl group (pKa 8.2) at C6 indicates that OFL can exist in aqueous solutions, as cation, zwitterion or anion depending on the pH of the solution. The monoprotonated cation, where the piperazinyl group is protonated, predominates in the pH range 2–4 and was used in this modeling study.

Initially, we performed molecular docking of the inclusion of OFL into HPβCD nano-cavity using *Autodock 4.2* [37]. By cluster analysis all complexes differing by 1.0 Å in a positional root mean square deviation (RMSD) were clustered together. The results show that the lowest energy structure (average $\Delta G = -6.50$ kcal mol^{-1}) for R-OFLX-HPβCD correspond to a frequency of 75 % whereas that of S-OFL-HPβCD the lowest energy structure (average $\Delta G = -6.55$ kcal mol^{-1}) correspond to 90 % of the of OFL conformation indicating convergence of the docking procedure for both systems. The predominant conformations of the inclusion complexes obtained for both enantiomers are shown in Fig. 5. It is evident from this figure that both enantiomers are introduced into the HPβCD through the secondary hydroxyl group side (wider side). This is expected as the side of cyclodextrin bearing the primary hydroxyl is affected by the steric blockage by the 2-hydroxypropyl substituents. It is clear that the large size of the fused ring system of OFL can easily fit into the extended and distorted CD cavity of HPβCD. These findings are in line with the reported NMR results [48]. In all cases the guest molecule is tilted towards the sides of the CD in order to maximize host–guest interactions such as hydrogen bonding.

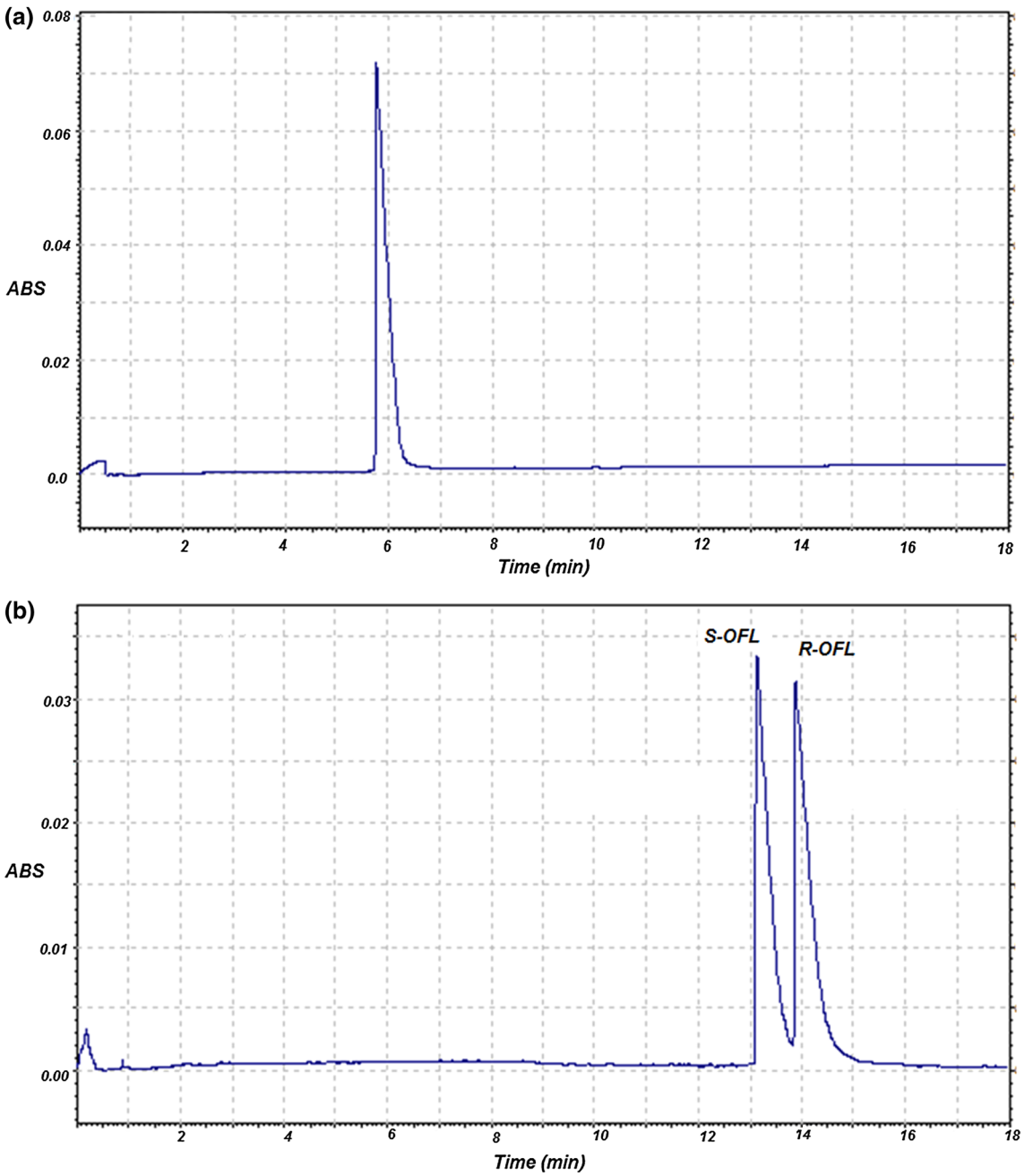

Fig. 2 Electropherogram obtained for the chiral separation of OFL using **a** βCD **b** HPβCD. Conditions: [Buffer], 50 mM; temperature, 25 °C; applied voltage, 15 kV

The differences in binding energies obtained by *Autodock* are insignificant compared to the standard errors reported for the docking simulations; therefore further calculations using the semiepirical PM7 were conducted. Quantum mechanical calculations were then performed on the structures of the complexes obtained from the docking simulation. We used the newly released PM7 method, a modified version of PM6 where errors associated with large molecules were reduced [36]. This method is used here to have further insight into the molecular recognition of OFL by HPβCD and to evaluate the energies and thermodynamic properties of the inclusion complexes more accurately. To obtain the binding energies ($\Delta E_{binding}$) of the 1:1 inclusion complexes the following equation was used:

$$\Delta E_{binding} = E_{complex} - E_{OFL} - E_{HP\beta CD} \quad (1)$$

where $E_{complex}$, E_{OFL}, $E_{HP\beta CD}$ are the energies of the inclusion complex, the free OFL and the free HPβCD

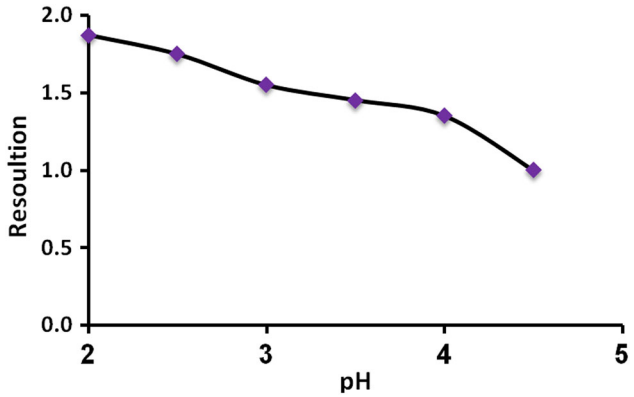

Fig. 3 Effect of pH on the resolution of OFL enantiomers. [HPβCD], 40 mM; [Buffer], 50 mM; voltage, 15 kV

molecules respectively. The calculated binding energies of OFL with HPβCD are given in Table 1. These results clearly show that interaction of guest with the host is associated with an energy that is always lower than the sum of the energies of the free molecules indicative of formation of stable inclusion complexes in both cases.

It is clear from Table 1 that the binding energy obtained by quantum mechanics calculations of HPβCD/R-OFL complex is higher than that of HPβCD/S-OFL by 15.0 kcal mol^{-1}. This result is in line with the CE experimental results indicating that a less stable complex is obtained with the S-OFL which travels faster through the column and therefore HPβCD efficiently separates the two enantiomers.

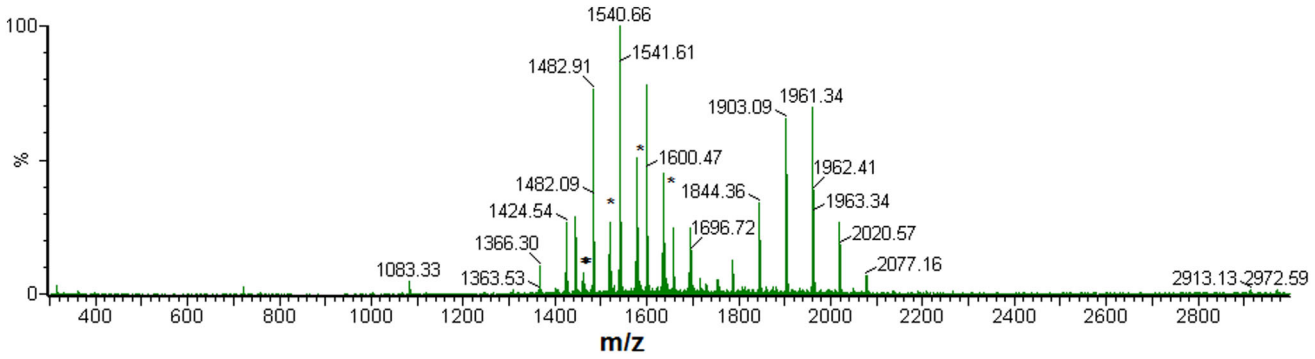

Fig. 4 ESI-MS spectrum of a mixture of OFL and HPβCD

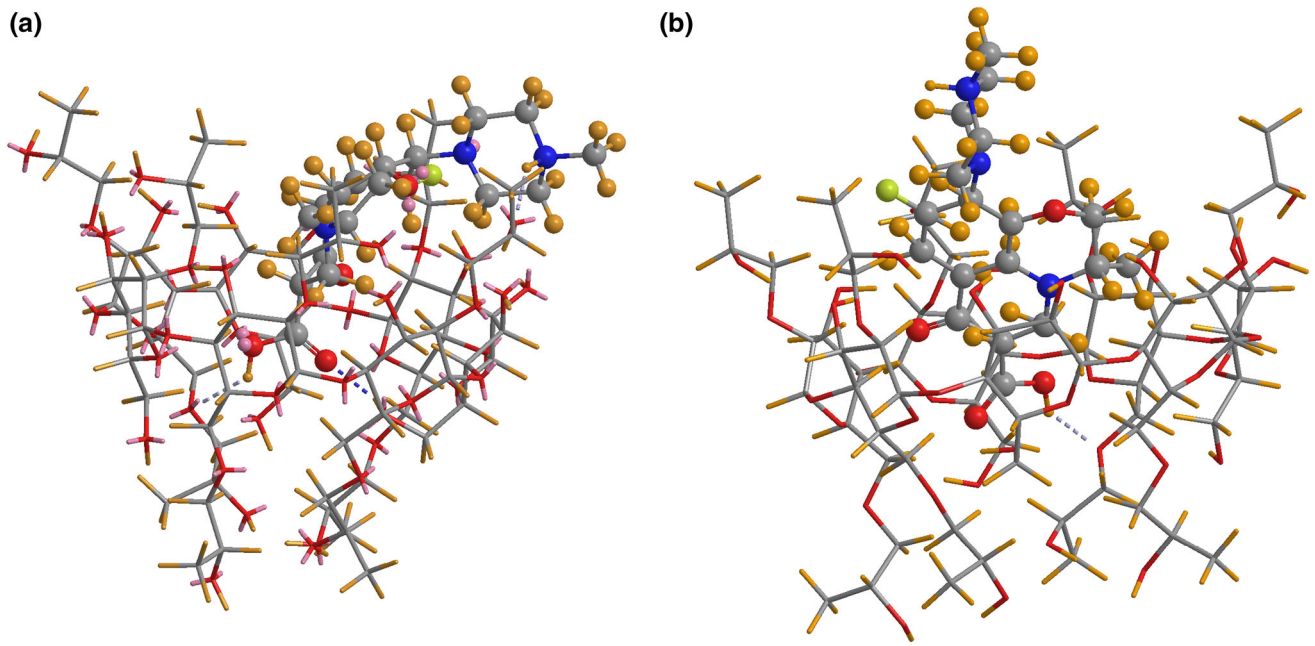

Fig. 5 Geometries of the inclusion complexes of **a** S-OFL-HPβCD **b** R-OFL-HPβCD

Table 1 Interaction energies and thermodynamic properties of OFLX-HPβCD inclusion complexes

Parameter	S-OFLX-HPβCD	R-OFLX-HPβCD
E (kcal mol^{-1})	−2193.0	−2207.0
ΔE (kcal mol^{-1})	−14.5	−29.5
ΔΔE (kcal mol^{-1})	15.0	
ΔH (kcal mol^{-1})	−16.7	−30.3
ΔS (cal $mol^{-1}K^{-1}$)	−41.7	−51.7
ΔG (kcal mol^{-1})	−4.3	−14.9

Using the parametric model PM7 we also performed statistical thermodynamic calculations at 1 atm and 298 K. The thermodynamic parameters, such as the enthalpy change (ΔH), entropy change (ΔS) and the Gibbs free energy change (ΔG) are summarized in Table 1 for the two complexes. The complex formation is clearly associated with a relatively large negative ΔH values indicating that it is enthalpically driven process. The replacement of high enthalpy water molecules from the cavity of the CD by suitable less polar molecules accompanied by formation of strong hydrophobic interaction remarkably lower the energy of the system. Deep insertion of guest molecules inside the host results in strong van der Waals effects, a process characterized by negative enthalpy changes and negative entropy changes. Similar results were experimentally obtained for the inclusion complex formation of OFL with βCD [49]. It was reported that the complexation was associated with an enthalpy change, ΔH, of −30.5 kcal mol^{-1} and an entropy change, ΔS, of −87.2 J mol^{-1} K^{-1}. These results are in line with those obtained by the theoretical procedure used in this study. Evidently, there are no simple models that could describe the mechanism of enantioseparation of racemic mixture by supramolecular assembly as it involves several forces working together such as hydrogen bonding, van der Waals interactions, release of ring strain and hydrophobic interactions among others.

MD simulation

In order to further rationalize recognition of R-OFL and S-OFL enantiomers by HPβCD and to have more insight into the mechanism of separation we have performed MD simulations on their complexes with HPβCD. These calculations are aimed at investigating the intermolecular interactions between the guest and the host molecules. In fact the analysis was focused on the hydrogen bond type of interactions. Nevertheless, in macrocycle molecules such as cyclodextrin guest molecules are customarily held strongly in the hydrophobic cavity by various interactions such as van der Waal forces, hydrophobic interactions and electrostatic forces, with hydrogen bonds playing a dominant role in enantiomer recognitions.

In this study 5 ns MD simulations were conducted in order to investigate the various structural features that contribute to the stability of the host–guest complexes of the drug with HPβCD. Analysis of these trajectories along the MD runs at constant temperature and pressure was performed showing that stable comcplexes were obtained. The root mean square deviations (rmsd) of the complexes conformations from a given reference frame were found to be stable after a simulation times of 1 ns for both systems (Fig. 6). The time evolutions of the distances from the center of mass of the macrocycle host and that of the drug ($d_{Cn–Cn}$) is shown in Fig. 7. Clearly, these results suggest that the relative placements of S-OFL and R-OFL guest molecule with respect to the host cavity are well preserved throughout the simulation time with values of $d_{Cn–Cn}$ of 1.7 ± 0.2 and 3.3 ± 0.5 Å for R-OFL and S-OFL, respectively. Moreover, the radius of gyration, r_{gyr}, was found to be 6.26 ± 0.07 and 6.48 ± 0.11 Å for S-OFL and R-OFL-HPβCD complexes, respectively. On the other hand, r_{gyr} values for HPβCD was found to be 6.50 ± 0.07 Å and that of OFL was 4.0 ± 0.04 Å. Inspection of these results reveals the fact that the values of r_{gyr} of the complexes are always lower than the sum of the two components and close to that of HPβCD indicating the formation of stable complexes during the simulation time. These results suggest that R-OFL forms a more stable complex with HPβCD compared to S-isomer.

We further investigated the H-bonding along the trajectories of the MD simulation for both complexes. The H-bond dynamics of the carboxyl groups of the two systems system is shown in Fig. 8. The distance between the carbonyl oxygen, O15, and the primary hydroxyl group of

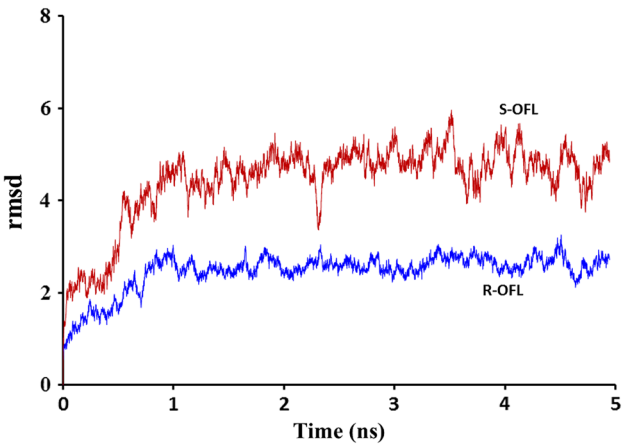

Fig. 6 RMSD plots for the simulation of R-OFL-HPβCD (*blue curve*), and S-OFL-HPβCD (*brown curve*). (Color figure online)

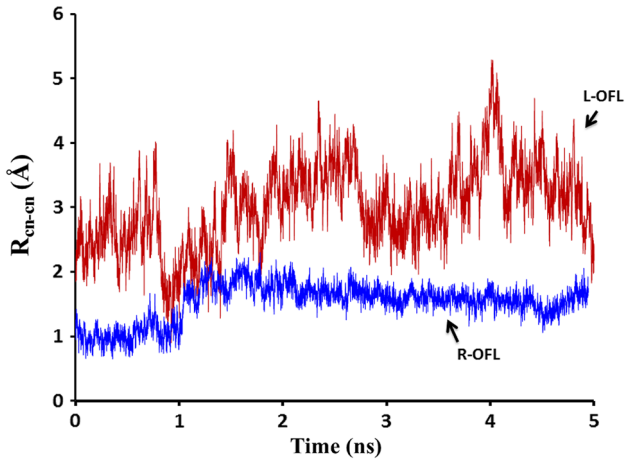

Fig. 7 Distance from the center of mass of OFL to that of the host molecule as a function of simulation time. R-OFL-HPβCD (*blue curve*), S-OFL-HPβCD (*brown curve*). (Color figure online)

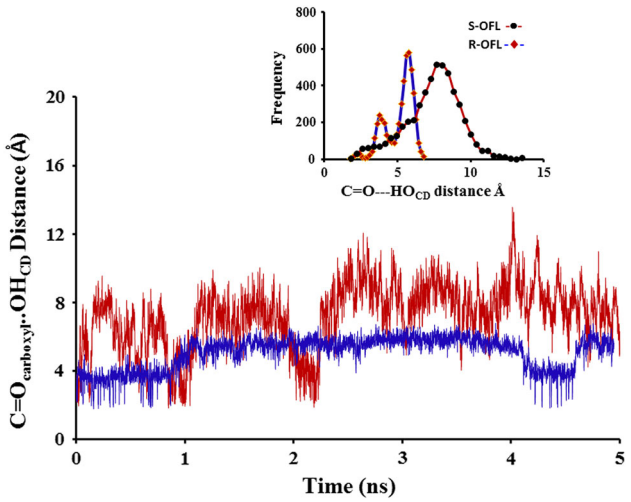

Fig. 8 Time evolution of the distance between O15 of OFL and the primary OH-groups on CD. R-OFL-HPβCD (*blue curve*), S-OFL-HPβCD (*brown curve*). *Inset* represents the distribution of $d_{O15–OH(CD)}$. (Color figure online)

the CD host fluctuates between 2 and 6 Å for R-OFL-HPβCD system and from 2 to 11 for S-OFL–HPβCD system. The bond distance of O15–OH_{CD} at the maximum distribution corresponds to 5.8 and 8.1 Å for R-OFL and S-OFL complexes, respectively. A similar trend is observed for the hydroxyl group of the guest (O17) interacting with the CD ether-oxygen atoms. These bond distances fluctuate around 4 Å during the first nanosecond then stabilized during the rest of the MD simulation at an average distance of 6 Å. These results, therefore, suggest that the carboxyl group of the guest molecules is present inside the cavity away from the sides of the host and is participating in minor hydrogen bonding interactions.

Interaction of O17 with neighboring OH groups on CD was also studied and the trajectories evolution is shown in Fig. 9. It is evident that hydrogen-bonding involving this group is not significant during the whole course of the simulation time. The distance at maximum distribution was found to be 4.0 and 4.8 Å for R-OFL and S-OFL complexes, respectively.

We also examined the evolution of various C–H–O bond distances with time. The role of such bonds in the bindings of single and double stranded nucleic acids, in protein interactions and in determining the packing of organic molecules is well documented in the literature [50, 51]. The existence of such H-bonds has been evidenced by spectroscopic and theoretical studies [50, 52, 53]. It is also believed that supramolecular assemblies are not only stabilized by strong hydrogen bonds, but also by many weak C–H–O bonds due to their electrostatic nature. For instance, X-ray crystallography studies of the inclusion complexes of 2, 7-dihydroxy-naphthalene have shown the presence of four C–H–O hydrogen bonds in addition to an O–H–O hydrogen bond and it was argued that these bonds contributed to the firm hold of the guest inside the host cavity [52]. However, the interaction effect of these C–H–O hydrogen bonds is known to diminish as solvents dielectric constant increases. Therefore, we strongly believe that these bonds play a considerable role in the host–guest interactions in solutions beside the O–H–O hydrogen bonds and other hydrogen bonds and consequently can be considered as an important factor in enantioseparations in guest–host systems.

Figure 10 shows the time evolution of the distance between the aromatic hydrogen (H of C8) of the guest

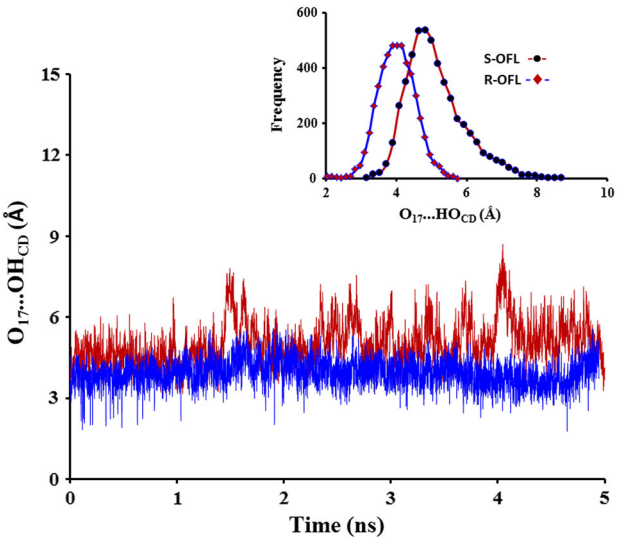

Fig. 9 Time evolution of the distance between OFL O17 and OH-groups on HPβCD. R-OFL-HPβCD (*blue curve*), S-OFL-HPβCD (*brown curve*). *Inset* Distribution of $d_{O17–OH(CD)}$. (Color figure online)

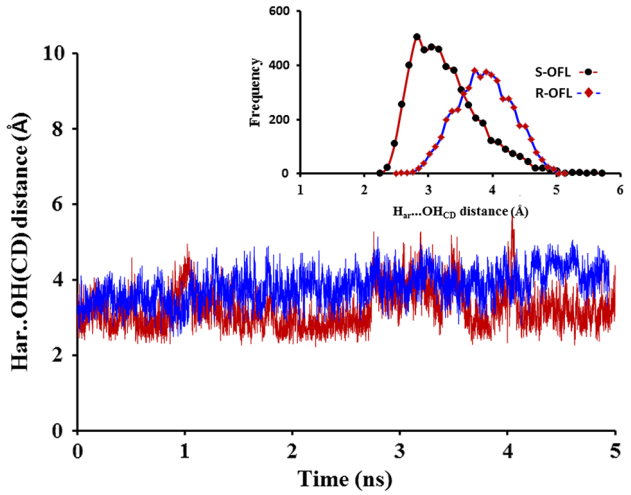

Fig. 10 Time evolution of the distance between aromatic hydrogen (H on C8) and OH-groups on HPβCD. R-OFL-HPβCD (*blue curve*), S-OFL-HPβCD (*brown curve*). *Inset* Distribution of $d_{Har–OH(CD)}$. (Color figure online)

molecules and the secondary OH– groups on the host molecule. Interestingly, as shown in the inset in this figure, the bond distance at the maximum distribution is shorter than 3.0 Å for S-OFL-HPβCD complex while that for R-OFL system is about 4.0 Å at the maximum distribution. This indicates that a weaker interaction is encountered with R-OFL inside the nanocavity of the host. However, these results also imply that R-OFL molecule is buried deeply in the CD cavity compared to S-OFL and therefore is not available for interaction with the secondary hydroxyl groups on the wider rim of the cyclodextrin.

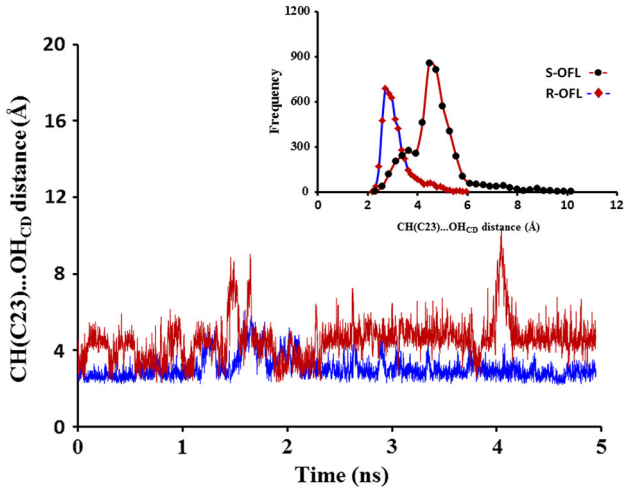

Fig. 11 Time evolution of the distance between H of C23 and secondary OH-groups on HPβCD. R-OFL-HPβCD (*blue curve*), S-OFL-HPβCD (*brown curve*). *Inset* Distribution of $d_{H(C23)–OHCD}$. (Color figure online)

The time evolution of interaction of the piperazine hydrogen atoms of C23 with the acceptor hydroxyl groups on the CD wider rim is shown in Fig. 11. The interaction between these hydrogen atoms and the oxygen of the secondary hydroxyl group on the CD is stronger for R-OFL complex compared to S-OFL complex as evident from the bond distance at the maximum distribution. At maximum distribution R-OFL complex shows a bond distance of 2.7 Å indicating that the guest enantiomer is forming reasonably strong C–H–O bond. In the case of S-OFL complex, the average bond distance increases to 4.5 Å indicating the formation of weaker interactions. Nevertheless, hydrogen bonds are dominated by electrostatic attraction their influence on polarization and charge transfer effects should not be ruled out. The soft carbonyl groups prefer to hydrogen bond with the soft donor C–H groups and are considered one of the best C–H–O hydrogen bond acceptor groups [51].

Clearly, the above results suggest that the tumbling of the molecule inside the host cavity is driven mainly by the tendency of these guest molecules to adopt stable interactions and to minimize steric effects. This in most of the cases is governed by the orientation of the various groups into the cavity of the host molecule. Consequently, this will eventually affect the chiral segregation of these species by the macrocycle host molecule. The above analyses have shown that in most of the cases R-OFL interacts more strongly with the guest molecule. Nevertheless, the separation of ofloxacin enantiomers is mainly governed by the stability of the inclusion complexes formed the effect of other factors, such as the variations of charge density and the size of the inclusion complex, on the separation cannot be neglected. It is worth noting here that quantification of such factors is not trivial and may require the use of the more computationally demanding quantum mechanics techniques.

Conclusion

Separation of enantiomers of ofloxacin has been achieved by using HPβCD in capillary electrophoresis and utilizing acidic buffers. An extensive theoretical study was conducted here to unravel the mechanism of the separation of the enantiomers of Ofloxacin. Using *Autodock* the most possible conformers of the S-OFL- and R-OFL-HPβCD were generated by molecular mechanics calculations. The optimum conformations generated by this technique were further optimized by the newly introduced PM7 semiempirical method. The theoretical results obtained here corroborated the experimental findings obtained by the capillary electrophoresis separation. R-OFL-HPβCD inclusion complex was found more stable compared to the

S-OFL-HPβCD inclusion complex, and therefore migrates at a slower veleocity towards the detector. The nature of bonding between the guest and host molecules was investigated using molecular dynamic simulations in aqueous media. The results obtained here indicated that these complexes are stabilized by weak hydrogen bonds between guest and host molecules. The role of the C–H–O bonds was also investigated and our findings indicate that this type of hydrogen bonding are of significant importance in enantiomer separation involving supramolecular systems.

References

1. Zhao, M., Cui, Y., Yu, J., Xu, S., Guo, X.: Combined use of hydroxypropyl-β-cyclodextrin and ionic liquids for the simultaneous enantioseparation of four azole antifungals by CE and a study of the synergistic effect. J. Sep. Sci. **37**, 151 (2014)
2. Chen, B., Zhang, Y., Xie, H.L., Chen, Q.M., Mai, Q.H.: Chiral separation of ofloxacin enantiomers by microchip capillary electrophoresis with capacitively coupled contactless conductivity detection. J. Chin. Chem. Soc. **61**, 432 (2014)
3. Jáč, P., Scriba, G.K.E.: Recent advances in electrodriven enantioseparations. J. Sep. Sci. **36**, 52 (2013)
4. Elbashir, A.A., Aboul-Enein, H.Y.: Capillary electrophoresis and molecular modeling as a complementary technique for chiral recognition mechanism. Crit. Rev. Anal. Chem. **43**, 131 (2013)
5. Scriba, G.K.E.: Fundamental aspects of chiral electromigration techniques and application in pharmaceutical and biomedical analysis. J. Pharm. Biomed. Anal. **55**, 688 (2011)
6. Dixit, S., Park, J.H.: Application of antibiotics as chiral selectors for capillary electrophoretic enantioseparation of pharmaceuticals: a review. Biomed. Chromatogr. **28**, 10 (2014)
7. Domínguez-Vega, E., Pérez-Fernández, V., Crego, A.L., García, M.Á., Marina, M.L.: Recent advances in CE analysis of antibiotics and its use as chiral selectors. Electrophoresis **35**, 28 (2014)
8. Tsioupi, D.A., Stefan-vanStaden, R.-I., Christodoulou, C.P.K.: Chiral selectors in CE: recent developments and applications. Electrophoresis **34**, 178 (2013)
9. Mangelings, D., Vander, Heyden Y.: Enantioselective capillary electrochromatography: recent developments and new trends. Electrophoresis **32**, 2583 (2011)
10. Al Azzam, K.M., Saad, B., Adnan, R., Aboul-Enein, H.Y.: Enantioselective analysis of ofloxacin and ornidazole in pharmaceutical formulations by capillary electrophoresis using single chiral selector and computational calculation of their inclusion complexes. Anal. Chim. Acta **674**, 249 (2010)
11. Mofaddel, N., Krajian, H., Villemin, D., Desbane, P.L.: Enantioseparation of binaphthol and its mono derivatives by cyclodextrin-modified capillary zone electrophoresis. J. Chromatogr. A **1211**, 142 (2008)
12. Juvancz, Z., Kendrovics, R.B., Iványi, R., Szente, L.: The role of cyclodextrins in chiral capillary electrophoresis. Electrophoresis **29**, 1701 (2008)
13. Scriba, G.K.E.V.: Cyclodextrins in capillary electrophoresis enantioseparations—recent developments and applications. J. Sep. Sci. **31**, 1991 (2008)
14. Chankvetadze, B.: Enantioseparations by using capillary electrophoretic techniques. The story of 20 and a few more years. J. Chromatogr. A **1168**, 45 (2007)
15. Chankvetadze, B., Lindner, W., Scriba, G.K.E.: Enantiomer separations in capillary electrophoresis in the case of equal binding constants of the enantiomers with a chiral selector: commentary on the feasibility of the concept. Anal. Chem. **76**, 4256 (2004)
16. Rizzi, A.: Fundamental aspects of chiral separations by capillary electrophoresis. Electrophoresis **22**, 3079 (2001)
17. Rizzi, A.M., Kremser, L.: pKa shift-associated effects in enantioseparations by cyclodextrin-mediated capillary zone electrophoresis. Electrophoresis **20**, 2715 (1999)
18. Elbashir, A.A., Suliman, F.O.: Computational modeling of capillary electrophoretic behavior of primary amines using dual system of 18-crown-6 and β-cyclodextrin. J. Chromatogr. A **1218**, 5344 (2011)
19. Prapasawat, T., Lothongkum, A.W., Pancharoen, U.: Modelling and experimental validation of enantioseparation of racemic phenylalanine via a hollow fibre-supported liquid membrane. Chem. Papers **68**, 180 (2014)
20. Ortuso, F., Alcaro, S., Menta, S., Fioravanti, R., Cirilli, R.: A chromatographic and computational study on the driving force operating in the exceptionally large enantioseparation of *N*-thiocarbamoyl-3-(4′-biphenyl)-5-phenyl-4,5-dihydro-(1H) pyrazole on a 4-methylbenzoate cellulose-based chiral stationary phase. J. Chromatogr. A **1324**, 71 (2014)
21. Shi, J.H., Su, Y.H., Jiang, W.: Enantioseparation and chiral recognition of a-cyclohexylmandelic acid and methyl a-cyclohexylmandelate on hydroxypropyl-b-cyclodextrin as chiral selector: HPLC and molecular modeling. J. Chromatogr. Sci. **51**, 8 (2013)
22. Suliman, F.O., Elbashir, A.A.: Enantiodifferentiation of chiral baclofen by β-cyclodextrin using capillary electrophoresis: a molecular modeling approach. J. Mol. Struct. **1019**, 43 (2012)
23. Li, W., Tan, G., Zhao, L., Chen, X., Zhang, X., Zhu, Z., Chai, Y.: Computer-aided molecular modeling study of enantioseparation of iodiconazole and structurally related triadimenol analogues by capillary electrophoresis: chiral recognition mechanism and mathematical model for predicting chiral separation. Anal. Chim. Acta **718**, 138 (2012)
24. Li, W., Liu, C., Tan, G., Zhang, X., Zhu, Z., Chai, Y.: Molecular modeling study of chiral separation and recognition mechanism of b-adrenergic antagonists by capillary electrophoresis. Int. J. Mol. Sci. **13**, 710 (2012)
25. Shi, J.H., Ding, Z.J., Hu, Y.: Experimental and theoretical studies on the enantioseparation and chiral recognition of mandelate and cyclohexylmandelate on permethylated β-Cyclodextrin chiral stationary phase. Chromatographia **74**, 319 (2011)
26. Bikádi, Z., Fodor, G., Hazai, I., Hári, P., Szemán, J., Szente, L., Fülöp, F., Péter, A., Hazai, E.: Molecular modeling of enantioseparation of phenylazetidin derivatives by cyclodextrins. Chromatographia **71**, S21 (2010)
27. Varghese, B., Al-Busafi, S.N., Suliman, F.O., Al-Kindy, S.M.Z.: Study on the spectral and inclusion properties of a sensitive dye, 3-naphthyl-1-phenyl-5-(5-fluoro-2-nitrophenyl)-2-pyrazoline, in solvents and β-cyclodextrin. Spectrochimica Acta Part A **136**, 661 (2015)
28. Zimnicka, M., Troć, A., Ceborska, M., Jakubczak, M., Koliński, M., Danikiewicz, W.: Structural elucidation of specific noncovalent association of folic acid with native cyclodextrins using an ion mobility mass spectrometry and theoretical approach. Anal. Chem. **86**, 4249 (2014)
29. Rajendiran, N., Mohandoss, T., Venkatesh, G.: nvestigation of inclusion complexes of sulfamerazine with α- and β-cyclodextrins: an experimental and theoretical study. Spectrochimica Acta Part A **124**, 441 (2014)
30. Asensi-Bernardi, L., Escuder-Gilabert, L., Martin-Biosca, Y., Medina-Hernandez, M.J., Sagrado, S.: Modeling the chiral resolution ability of highly sulfated b-cyclodextrin for basic compounds in electrokinetic chromatography. J. Chromatogr. A **1308**, 152 (2013)

31. Eid, E.E., Abdul, A.B., Suliman, F.O., Sukari, M.A., Rasedee, A., Fatah, S.S.: Characterization of the inclusion complex of zerumbone with hydroxypropyl-β-cyclodextrin. Carbohydr. Polym. **83**, 1707 (2011)
32. Toth, G., Mohacsi, R., Racz, A., Rusu, A., Horvath, P., Szente, L., Beni, S., Noszai, B.: Equilibrium and structural characterization of ofloxacin-cyclodextrin complexation. J. Incl. Phenom. Macrocycl. Chem. **77**, 291 (2013)
33. Elbashir, A.A., Saad, B., Aboul-Enein, H.Y.: Recent developments of enantioseparations for fluoroquinolones drugs using liquid chromatography and capillary electrophoresis. Curr. Pharm. Anal. **6**, 246 (2010)
34. Yan, H., Row, K.H.: Rapid chiral separation and impurity determination of levofloxacin by ligand-exchange chromatography. Anal. Chim. Acta **584**, 160 (2007)
35. Zhou, S., Ouyang, J., Baeyens, W.R.G., Zhao, H., Yang, Y.: Chiral separation of four fluoroquinolone compounds using capillary electrophoresis with hydroxypropyl-βcyclodextrin as chiral selector. J. Chromatogr. A **1130**, 296 (2006)
36. Stewart, J.J.P.: Optimization of parameters for semiempirical methods VI: more modifications to the NDDO approximations and re-optimization of parameters. J. Mol. Model. **19**, 1 (2013)
37. Morris, G.M., Goodsell, D.S., Halliday, R.S., Huey, R., Hart, W.E., Belew, R.K., Olson, A.J.: In. The Scripps Research Institute, La Jolla (2009)
38. Sanner, M.F., Huey, R., Dallakyan, S., Lindstorm, W., Morris, G.M., Norledge, A., Omelchenko, A., Stoffler, D., Vareille, G.: In. The Scripps Institute, La Jolla (2007)
39. Gasteiger, J., Marsili, M.: Iterative partial equalization of orbital electronegativity—a rapid access to atomic charges. Tetrahedron **36**, 3219 (1980)
40. Jorgensen, W.L., Chandrasekhar, J., Madura, J.D., Impey, R.W., Klein, M.L.: Comparison of simple potential functions for simulating liquid water. J. Chem. Phys. **79**, 926 (1983)
41. Phillips, J.C., Braun, R., Wang, W., Gumbart, J., Tajkhorshid, E., Villa, E., Chipot, C., Skeel, R.D., Kale, L., Schulten, K.: Scalable molecular dynamics with NAMD. J. Comput. Chem. **26**, 1781 (2005)
42. MacKerell Jr, A.D., Bashford, D., Bellott, M., Dunbrack Jr, R.L., Evanseck, J.D., Field, M.J., Fischer, S., Gao, J., Guo, H., Ha, S., Joseph-McCarthy, D., Kuchnir, L., Kuczera, K., Lau, F.T.K., Mattos, C., Michnick, S., Ngo, T., Nguyen, D.T., Prodhom, B., Reiher, W.E., Roux, B., Schlenkrich, M., Smith, J.C., Stote, R., Straub, J., Watanabe, M., Wiórkiewicz-Kuczera, J., Yin, D., Karplus, M.: All-atom empirical potential for molecular modeling and dynamics studies of proteins. J. Phys. Chem. B **102**, 3586 (1998)
43. Pedretti, A., Villa, L., Vistoli, G.: VEGA: a versatile program to convert, handle and visulize molecular structure on Windows-based PCs. J. Mol. Graph. Model. **21**, 47 (2002)
44. Humphrey, W., Dalke, A., Schulten, K.: VMD—visual molecular dynamics. J. Mol. Graph. Model. **14**, 33 (1996)
45. Rao, C.T., Pitha, J., Lindberg, B., Lindberg, J.: Distribution of substituents in O-(2-hydroxypropyl) derivatives of cyclomaltooligosaccharides (cyclodextrins): influence of increasing substitution, of the base used in the preparation, and of macrocyclic size. Carbohydr. Res. **223**, 99 (1992)
46. Rusu, A., Tóth, G., Szőcs, L., Kökösi, J., Kraszni, M., Gyéresi, Á., Noszál, B.: Triprotic site-specific acid–base equilibria and related properties of fluoroquinolone antibacterials original research article. J. Pharm. Biomed. Anal. **66**, 50 (2012)
47. Babić, S., Horvat, A.J.M., Pavlović, D.M., Kaštelan-Macan, M.: Determination of pKa values of active pharmaceutical ingredients. Trends Anal. Chem. **26**, 1043 (2007)
48. Li, J., Zhang, X.: Preparation and characterization of the inclusion complex ofofloxacin with bCD and HP-bCD. J. Incl. Phenom. Macrocycl. Chem. **69**, 173 (2011)
49. Ghosh, B.C., Deb, N., Mukherjee, A.K.: Determination of individual proton affinities of ofloxacin from its UV − Vis absorption, fluorescence and charge-transfer spectra: effect of inclusion in β-cyclodextrin on the proton affinities. J. Phys. Chem. B **114**, 9862 (2010)
50. Raymo, F.M., Bartberger, M.D., Houk, K.N., Stoddart, J.F.: The magnitude of [C–H···O] hydrogen bonding in molecular and supramolecular assemblies. J. Am. Chem. Soc. **123**, 9264 (2001)
51. Desiraju, G.R.: The C–H···O hydrogen bond: structural implications and supramolecular design. Acc. Chem. Res. **29**, 441 (1996)
52. Añibarro, M., Geßler, K., Usón, I., Sheldrick, G.M., Saenger, W.: X-ray structure of β-cyclodextrin-2,7-dihydroxy-naphthalene·4.6 H2O: an unusually distorted macrocycle. Carbohydr. Res. **333**, 251 (2001)
53. Nakagawa, T., Immel, S., Lichtenthaler, F.W., Lindner, H.J.: Topography of the 1:1 α-cyclodextrin–nitromethane inclusion complex. Carbohydr. Res. **324**, 141 (2000)